Journal of Microbiology (2014) Vol. 52, No. 1, pp. 53–63
DOI 10.1007/s12275-014-3410-z

Application of Statistical Experimental Design for Optimization of Silver Nanoparticles Biosynthesis by a Nanofactory *Streptomyces viridochromogenes*

Noura El-Ahmady El-Naggar[1]* and Nayera A.M. Abdelwahed[2]

[1]*Department of Bioprocess Development, Genetic Engineering and Biotechnology Research Institute, City of Scientific Research and Technological Applications, Alexandria 21934, Egypt*
[2]*Chemistry of Natural and Microbial Products Dept., National Research Center,12311, Dokki, Cairo, Egypt*

(Received Jul 31, 2013 / Revised Sep 2, 2013 / Accepted Sep 3, 2013)

Central composite design was chosen to determine the combined effects of four process variables ($AgNO_3$ concentration, incubation period, pH level and inoculum size) on the extracellular biosynthesis of silver nanoparticles (AgNPs) by *Streptomyces viridochromogenes*. Statistical analysis of the results showed that incubation period, initial pH level and inoculum size had significant effects ($P<0.05$) on the biosynthesis of silver nanoparticles at their individual level. The maximum biosynthesis of silver nanoparticles was achieved at a concentration of 0.5% (v/v) of 1 mM $AgNO_3$, incubation period of 96 h, initial pH of 9 and inoculum size of 2% (v/v). After optimization, the biosynthesis of silver nanoparticles was improved by approximately 5-fold as compared to that of the unoptimized conditions. The synthetic process of silver nanoparticle generation using the reduction of aqueous Ag+ ion by the culture supernatants of *S. viridochromogenes* was quite fast, and silver nanoparticles were formed immediately by the addition of $AgNO_3$ solution (1 mM) to the cell-free supernatant. Initial characterization of silver nanoparticles was performed by visual observation of color change from yellow to intense brown color. UV-visible spectrophotometry for measuring surface plasmon resonance showed a single absorption peak at 400 nm, which confirmed the presence of silver nanoparticles. Fourier Transform Infrared Spectroscopy analysis provided evidence for proteins as possible reducing and capping agents for stabilizing the nanoparticles. Transmission Electron Microscopy revealed the extracellular formation of spherical silver nanoparticles in the size range of 2.15–7.27 nm. Compared to the cell-free supernatant, the biosynthesized AgNPs revealed superior antimicrobial activity against Gram-negative, Gram-positive bacterial strains and *Candida albicans*.

***Keywords*:** biosynthesis, silver nanoparticles, antimicrobial activity, *Streptomyces viridochromogenes*, transmission electron microscope, response surface methodology

*For correspondence. E-mail: nouraelahmady@yahoo.com; Tel.: +002-01 003738444; Fax: +002-034593423

Introduction

Nanotechnology involves the production, manipulation and use of materials which are less than a micron in size (Mohanpuria *et al.*, 2008). In recent years, there has been growing interest in the manufacture of silver nanoparticles. Silver, in its metallic as well as ionic forms, exhibits cytotoxicity against several microorganisms, and hence, is used as an antimicrobial agent (Valodkar *et al.*, 2010) in surgically implanted catheters in order to reduce infections caused during surgery, and has been proposed to possess anti-fungal, anti-inflammatory, antiangiogenic and anti-permeability activities (Kalishwaralal *et al.*, 2009, 2010), as well as being currently used as an antibacterial agent in food storage and textiles. Silver nanoparticles are also used in hygienic products including water purification systems, linings of washing machines, dishwashers, refrigerators, and toilet seats (Rai *et al.*, 2009), in addition to numerous industrial applications, including heterogeneous catalysis, cosmetics, microelectronics, conductive inks and adhesives (Akaighe *et al.*, 2011). Biologically synthesized silver nanoparticles could have many applications, as in spectrally selected coatings for solar energy absorption, as intercalation materials for electrical batteries, as optical receptors, as catalysts in chemical reactions, as antimicrobials, and in bio-labeling (Souza *et al.*, 2004). An important aspect of nanotechnology is the development of toxicity-free synthesis of metal nanoparticles, which is a great challenge. The chemical synthesis of nanoparticles has adverse effects due to the use of toxic-reducing agents, which pose potential risks to human health and the environment. Hence, there is an ever-growing need to develop inexpensive, clean, nontoxic, large scale and environmentally safe synthesis procedures. The microbial mediated biosynthesis of nanomaterials has recently been recognized as a promising source for mining nanomaterials (Verma *et al.*, 2009). Biosynthetic methods can be categorized into intracellular and extracellular synthesis, according to the location where nanoparticles are formed in relation to the cell (Ahmad *et al.*, 2010; Tang *et al.*, 2011). It has been well documented that silver nanoparticle production is possible using certain bacteria, fungi, and yeast strains. However, microbe-specific variation in nanoparticle properties has been observed (Vigneshwaran *et al.*, 2006; Sanghi and Verma, 2009). For example, the time required for completion of nanoparticle production varies from 24 to 120 h. In addition, the size, sta-

bility, and dispersion properties of produced nanoparticles varied with the type of microbial strain employed (pyramidal, spherical shaped particles), indicating that the biochemical and genetic nature of microbial strains employed, plays a significant role in controlling the nanoparticle biogenic processes (Hemanth Naveen *et al.*, 2010).

Optimization of medium components and cultural parameters is the primary task in a biological process (Djekrif-Dakhmouche *et al.*, 2006). Fermentation processes have been optimized by changing one independent variable or factor at a time, while keeping the others at some fixed values. Single variable optimization methods are not only tedious, time consuming, laborious and expensive but can also lead to a misinterpretation of results, especially because the interaction effects among different factors are overlooked (Wenster-Botz, 2000). Limitations of the single factor optimization can be eliminated by employing response surface methodology (RSM) which is used to explain the combined effects of all the factors in a fermentation process (Elibol, 2004). Response surface methodology is a statistical technique, based on the fundamental principles of statistics, randomization, replication and duplication, which simplifies the optimization by studying the mutual interactions among the variables over a range of values in a statistically valid manner. It is an efficient statistical technique for the optimization of multiple variables in order to predict the best performance conditions with a minimum number of experiments, and can explain the individual and interactive effects of test variables on the response (Panwal *et al.*, 2011).

The aim of the present study was to optimize the green synthesis of silver nanoparticles by *Streptomyces viridochromogenes* using response surface methodology. The biosynthesized silver nanoparticles were characterized using a UV-VIS spectrophotometer, transmission electron microscope (TEM), Fourier Transform Infra-Red (FTIR) spectroscopy analysis and Energy dispersive X-ray (EDX) spectroscopy analysis, in addition to antimicrobial properties using Gram-positive, Gram-negative bacterial strains and yeast.

Materials and Methods

Microorganisms and cultural conditions

Seven *Streptomyces* isolates were kindly provided by Dr. Noura El-Ahmady El-Naggar (Department of Bioprocess Development, Genetic Engineering and Biotechnology Research Institute, City of Scientific Research and Technological Applications, Alexandria, Egypt). These isolates were maintained on slopes containing starch-nitrate agar medium (Waksman, 1959) of the following composition (g/L): Starch 20; KNO_3 2 ; K_2HPO_4 1; $MgSO_4{\cdot}7H_2O$ 0.5; NaCl 0.5; $CaCO_3$ 3; $FeSO_4{\cdot}7H_2O$ 0.01; agar 20 and distilled water up to 1 L. Slopes were incubated for a period of 7 days at 30°C. The isolates were stored as spore suspensions in 20% (v/v) glycerol at -20°C for subsequent investigation.

Inoculum preparation

250 ml Erlenmeyer flasks containing 50 ml of medium consisting of g/L: Soluble starch 20; $NaNO_3$ 2; K_2HPO_4 1; $MgSO_4{\cdot}7H_2O$ 0.5 and distilled water up to 1 L were inoculated with three disks of 9 mm diameter taken from a 7-days old stock culture grown on starch nitrate agar medium. The flasks were incubated for 48 h in a rotatory incubator shaker at 30°C and 200 rpm, and were used as an inoculum for subsequent experiments.

Extracellular synthesis of AgNPs

In order to screen for an efficient strain for the synthesis of AgNPs, 7 *Streptomyces* isolates were freshly inoculated in an Erlenmeyer flask containing 50 ml of the production medium consisting of g/L: Soluble starch 20; $NaNO_3$ 2; K_2HPO_4 1; $MgSO_4{\cdot}7\ H_2O$ 0.5 and distilled water up to 1 L. The inoculated flasks were incubated on a rotatory incubator shaker at 30°C and 200 rpm for 72 h. After the incubation period, the cell free supernatant was obtained by centrifugation at 5,000 rpm for 30 min. For the biosynthesis of AgNPs to occur, 1% (v/v) of 1 mM $AgNO_3$ was added to cell free supernatant and was incubated on an orbital shaker (dark condition) for 24 h at 30°C. The cell free supernatant without the addition of $AgNO_3$ was maintained as a control. Consequently, the bio reduction reaction was monitored by visual color change and UV-visible absorbance of the reaction mixture in the 300–600 nm range. Based on the rapid reduction of $AgNO_3$ into AgNPs, a proficient *Streptomyces* strain was selected and used for further characterization.

Experimental design

In this study, the effect of four process parameters, namely $AgNO_3$ concentration (X_1), incubation period (X_2), pH level (X_3) and inoculum size (X_4) on the biosynthesis of silver nanoparticles was studied and optimized using central composite design (CCD). Each factor in the design was studied at five different levels (-2, -1, 0, 1, 2). The central values (zero level) chosen for experimental design were: 1 mM $AgNO_3$ 1% (v/v), incubation period 72 h, pH level 8 and inoculum size 4% (v/v). The experimental design used for the study consisted of 30 trials (Table 1). Experiments were conducted in 250 ml Erlenmeyer flask containing 50 ml of medium prepared according to the design. The flasks were kept in an incubator shaker which was maintained at 30°C and 200 rpm.

All the experiments were carried out in duplicate and the average of absorbance at 400 nm which indicated the biosynthesis of silver nanoparticles was taken as the dependent variable or response (Y).

The experimental results of CCD were fitted via the response surface regression procedure, using the following second order polynomial equation:

$$Y = \beta_0 + \sum_i \beta_i X_i + \sum_{ii} \beta_{ii} X_i^2 + \sum_{ij} \beta_{ij} X_i X_j \qquad \text{Equation (1)}$$

where Y is the predicted response, β_0 is the regression coefficients, β_i is the linear coefficient, β_{ii} is the quadratic coefficients, β_{ij} is the interaction coefficients) and Xi is the coded level of independent variables. In this study, the independent variables were coded as X_1, X_2, X_3, and X_4. Thus, the second order polynomial equation can be presented as follows:

Table 1. Full factorial central composite design matrix of four process variables, with actual factor levels corresponding to coded factor levels, and mean responses for the biosynthesis of silver nanoparticles by *S. viridochromogenes*

Run	$AgNO_3$, 1 mM (%, v/v)	Incubation period (h)	Initial pH level	Inoculum size (%, v/v)	Absorbance at 400 nm	
					Experimental	Predicted
1	0 (1)	2 (120)	0 (8)	0 (4)	1.438	1.269
2	-2 (0.2)	0 (72)	0 (8)	0 (4)	0.374	0.495
3	0 (1)	-2 (24)	0 (8)	0 (4)	0.105	0.281
4	2 (2)	0 (72)	0 (8)	0 (4)	0.497	0.383
5	0 (1)	0 (72)	2 (10)	0 (4)	1.488	1.531
6	0 (1)	0 (72)	0 (8)	0 (4)	0.395	0.395
7	0 (1)	0 (72)	-2 (6)	0 (4)	0.248	0.212
8	0 (1)	0 (72)	0 (8)	0 (4)	0.395	0.395
9	0 (1)	0 (72)	0 (8)	-2 (1)	0.504	0.501
10	0 (1)	0 (72)	0 (8)	2 (8)	0.279	0.289
11	1 (1.5)	1 (96)	-1 (7)	-1 (2)	0.285	0.384
12	1 (1.5)	-1 (48)	1 (9)	-1 (2)	0.822	0.770
13	1 (1.5)	1 (96)	-1 (7)	1 (6)	0.492	0.516
14	1 (1.5)	1 (96)	1 (9)	-1 (2)	0.948	1.079
15	0 (1)	0 (72)	0 (8)	0 (4)	0.395	0.395
16	-1 (0.5)	-1 (48)	-1 (7)	-1 (2)	0.037	0.004
17	1 (1.5)	-1 (48)	-1 (7)	1 (6)	0.129	0.218
18	0 (1)	0 (72)	0 (8)	0 (4)	0.395	0.395
19	-1 (0.5)	1 (96)	1 (9)	1 (6)	1.028	1.085
20	-1 (0.5)	-1 (48)	1 (9)	1 (6)	0.603	0.501
21	1 (1.5)	-1 (48)	1 (9)	1 (6)	0.83	0.792
22	-1 (0.5)	-1 (48)	-1 (7)	1 (6)	0.011	-0.124
23	-1 (0.5)	1 (96)	-1 (7)	1 (6)	0.507	0.555
24	-1 (0.5)	1 (96)	-1 (7)	-1 (2)	0.753	0.788
25	1 (1.5)	1 (96)	1 (9)	1 (6)	0.966	0.996
26	-1 (0.5)	1 (96)	1 (9)	-1 (2)	1.626	1.534
27	0 (1)	0 (72)	0 (8)	0 (4)	0.395	0.395
28	0 (1)	0 (72)	0 (8)	0 (4)	0.395	0.395
29	1 (1.5)	-1 (48)	-1 (7)	-1 (2)	0.041	-0.020
30	-1 (0.5)	-1 (48)	1 (9)	-1 (2)	0.871	0.844

$$Y = \beta_0 + \beta_1 x_1 + \beta_2 x_2 + \beta_3 x_3 + \beta_4 x_4 + \beta_{12} x_1 x_2 + \beta_{13} x_1 x_3 + \beta_{14} x_1 x_4 + \beta_{23} x_2 x_3 + \beta_{24} x_2 x_4 + \beta_{11} x_1^2 + \beta_{22} x_2^2 + \beta_{33} x_3^2 + \beta_{44} x_4^2 \quad \text{Equation (2)}$$

The graphical representation of the model equation results in response surface plots that represent the individual and interactive effects of test variables on the response.

Statistical analysis

The experimental data obtained was subjected to multiple linear regressions, using Microsoft Excel 2007 to evaluate the analysis of variance (ANOVA) and to estimate the main effect, *t*-value, *P*-value and confidence level. The student t-test was used to determine the significance of the parameters regression coefficients. The *P*-values were used as a tool to check the significance of the interaction effects, which in turn, may indicate the patterns of the interactions among the variables (Montgomery, 1991). The quality of fit of regression model was expressed via the correlation coefficient (R), the coefficient of determination (R^2) and the adjusted R^2, and its statistical significance was determined by an F-test. The optimal value of activity was estimated using the *solver* function of Microsoft Excel. The statistical software package, STATISTICA software (Version 8.0, StatSoft Inc., USA) was used to plot the three-dimensional surface plots, in order to illustrate the relationship between the responses and the experimental levels of each of the variables utilized in this study.

Characterization of silver nanoparticles

UV-visible spectral analysis: The biosynthesized silver nanoparticles using the cell free supernatant were monitored by changes in color. AgNPs was characterized by UV-vis spectrophotometer (Jenway UV/Visible-2605 spectrophotometer, England) scanning in the range of 300–600 nm, at regular intervals. Cell free supernatant without the addition of silver nitrate was used as a control throughout the experiment.

Electron microscopic analysis: The supernatant from the maximum time-point of production of silver nanoparticles was subjected to a transmission electron microscope (JEOL, JEM-100CX), at the Electron Microscope Unit, Faculty of Science, Alexandria University.

Fourier Transform Infra-Red (FTIR) spectroscopy analysis: The interaction between protein and AgNPs was analyzed by Fourier transform infrared spectroscopy. The synthesized

AgNPs sample was freeze dried and diluted with potassium bromide (in the ratio of 1:100) to make a pellet. The FTIR spectrum of samples was recorded on a FTIR instrument (Shimadzu FTIR-8400 S). The measurement was carried out in the range of 500–4000 cm^{-1} at a resolution of 1 cm^{-1}.

Energy dispersive X-ray (EDX) spectroscopy analysis: EDX was carried out with the scanning electron microscope Jeol JSM-6360 LA (at the Central Laboratory, City of Scientific Research and Technological Applications, Egypt) equipped with an EDAX detector operated at an accelerating voltage of 20 keV to perform elemental analysis.

Antimicrobial activity of AgNPs by agar diffusion method

Antimicrobial activity was tested for biosynthesized AgNPs and cell free supernatant against bacterial pathogens of Gram-positive (*Staphylococcus aureus*), Gram-negative bacteria (*Pseudomonas aeruginosa*) and yeast (*Candida albicans*) using the well-diffusion method on Luria Bertani (LB) agar plates. A 100 µl bacterial suspension of each bacterial test organism was used to prepare bacterial lawns. Agar wells of 9 mm diameter were prepared with the help of a sterilized stainless steel cork borer. The wells were loaded with 100 µl of Ag nanoparticles solution and 100 µl of culture broth from *S. viridochromogenes* cell free supernatant without $AgNO_3$ as a control. The plates were incubated at 30°C for 24 h and were then examined for the presence of zones of inhibition. The diameter of such zones of inhibition was measured and the mean value for each organism was recorded and expressed in millimeters.

Results and Discussion

Evaluation of biosynthesis of silver nanoparticles by *Streptomyces* isolates

Seven *Streptomyces* isolates were evaluated for their extracellular silver nanoparticles biosynthesis. Out of 7 isolates, three isolates had the potential to reduce the silver ions to silver nanoparticles. Among the isolates, a strain that exhibited the rapid production of AgNPs, was identified as *Streptomyces viridochromogenes* (El-Naggar *et al.*, 2011). The biosynthesis of silver nanoparticles was indicated by the immediate change of the yellow colored reaction mixture to dark brown after the addition of 1 % (v/v) 1 mM aqueous $AgNO_3$ to the cell free supernatant of *S. viridochromogenes*. The reaction mixture was kept in the dark to avoid photolytic reaction. In contrast, there was no color change observed in aqueous $AgNO_3$ incubated without cell free supernatant under the same conditions (Fig. 1). The color formation is dependent on the excitation of surface Plasmon vibrations of silver nanoparticles (Ganesh Babu and Gunasekaran, 2009).

AgNPs are best formed in darkness (Minaeian *et al.*, 2008; Natarajan *et al.*, 2010), but it is still not known how darkness influences the formation of AgNPs. It has been suggested that DNA (Feng *et al.*, 2000), sulfur-containing proteins (Morones *et al.*, 2005) and NADH-dependent nitrate reductase (Ahmad *et al.*, 2003; Kalimuthu *et al.*, 2008) are involved in the synthesis of AgNPs by the bioreduction of silver ions to metallic silver. An NADH-dependent reductase is the main factor responsible for biosynthesis processes. This reductase gains electrons from NADH and oxidizes it to NAD+. The enzyme is then oxidized by the simultaneous reduction of metal ions (Senapati *et al.*, 2005). This enzyme is induced by nitrate ions and reduces silver ions to metallic silver (Vaidyanathan *et al.*, 2010).

Fig. 1. Visible observation of AgNPs biosynthesis by *S. viridochromogenes*: (A) cell-free supernatant, (B) After exposure to (1 mM) $AgNO_3$ solution.

UV-Visible spectral analysis

The presence of nanoparticles was confirmed using scanning UV-visible spectrophotometry in the range of 300–600 nm. The specific surface plasmon resonance (SPR) spectra of silver nanoparticles produced by the *S. viridochromogenes* revealed an absorption peak at 400 nm (Fig. 2) indicating the presence of AgNPs. Brause *et al*. (2002) reported that the optical absorption spectra of metal nanoparticles are mainly dominated by surface plasmon resonance, and the absorption peak is related to particle size. The surface plasmon resonance peak of silver nanoparticles in aqueous solution shifts to longer wavelengths with increasing particle size. The position and shape of plasmon absorption of silver nanoclusters are strongly dependant on particle size, stabilizing molecules or surface adsorbed particles, as well as the dielectric constant of the medium (Krishnaraj *et al.*, 2010). According to Mie's theory (Mie, 1908), only a single SPR band is expected in the absorption spectra of spherical nanoparticles, whereas anisotropic particles could give rise to two

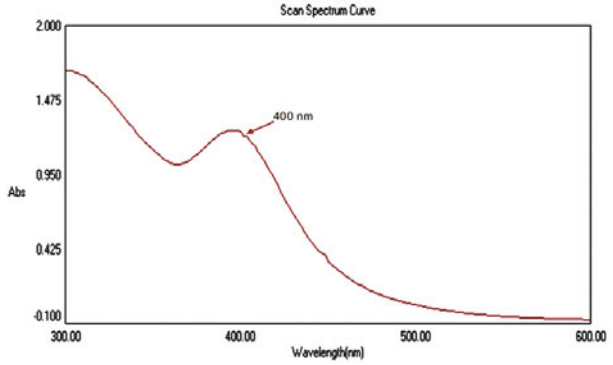

Fig. 2. UV-Vis absorption spectrum of silver nanoparticles synthesized by cell free supernatant of *S. viridochromogenes*. The absorption spectrum of silver nanoparticles exhibited a strong broad peak at 400 nm, and observation of such a band is assigned to surface Plasmon resonance of the particles.

Table 2. **Analysis of variance (ANOVA) for optimization of silver nanoparticles biosynthesis using central composite design**

	df	SS	MS	F-test	Significance F (*P*-value)
Regression	14.000	5.094	0.364	30.210	0.000
Residual	15.000	0.181	0.012		
Total	29.000	5.275			

df, Degree of freedom; SS, Sum of squares; MS, Mean sum of squares; F, Fishers's function; Significance F, Corresponding level of significance.

or more SPR bands depending on the shape of the particles. The number of SPR peaks increases as the symmetry of the nanoparticle decreases (Sosa *et al.*, 2003). In the present investigation, the reaction mixture showed a single SPR band at 400 nm revealing spherical shape of AgNPs, which was further confirmed by TEM images.

Optimization of silver nanoparticles biosynthesis using response surface methodology

In this study, a total of 30 experiments with different combination of $AgNO_3$ concentration (X_1), incubation period (X_2), initial pH (X_3), and inoculum size (X_4) were performed, and the results of experiments are represented in Table 1. Treatment runs 1, 5, and 26 showed a high silver nanoparticles biosynthesis (>1.4). The maximum silver nanoparticles biosynthesis (1.626) was achieved in the run number 26 under the conditions of 1 m $MAgNO_3$ (0.5%, v/v), incubation period (96 h), initial pH (9), and inoculum size (2%, v/v).

By applying multiple regression analysis to experimental data of central composite design (CCD), a second-order polynomial model explains the role of each variable and their second-order interactions on silver nanoparticles biosynthesis.

The determination coefficient (R^2) values provide a measure of how much variability in the observed response values can be explained by the experimental factors and their interactions. The R^2 value is always between 0 and 1. The closer the R^2 value is to 1, the stronger the model is, and the better it predicts the response (Kaushik *et al.*, 2006). The determination coefficient (R^2) of the model was 0.9657 indicating that 96.57% of variability in the response could be explained by the model. A regression model having an R^2-value higher than 0.9 is considered to have a very high correlation (Chen *et al.*, 2009). Therefore, the present R^2-value indicates a very good fit between the observed and predicted responses, and implies that the model is reliable for silver nanoparticles biosynthesis in the present study. In addition, the value of the adjusted determination coefficient (Adj. R^2=0.9338) is also very high, which indicates a high significance of the model (Akhnazarova and Kafarov, 1982). A higher value of the correlation coefficient (R=0.9827) signifies an excellent correlation between the independent variables, this indicates a good correlation between the experimental and predicted values (Box *et al.*, 1978). Thus, the analysis of the response trend using the model was considered to be reasonable.

The results of the second order response surface model fitting in the form of analysis of variance (ANOVA) are given in Table 2. ANOVA is required to test the significance and adequacy of the model. The Fisher variance ratio, the *F*-value, which is a statistically valid measure of how well the factors describe the variation in the data about its mean. The analysis of variance (ANOVA) of the regression model demonstrates that the model is highly appropriate, as is evident from the Fisher's *F*-test (30.210) and a very low probability value (0.000).

All values of model coefficients were calculated by multiple regression analysis. The significance of each coefficient was determined by the Student's *t*-test and *P*-values, as listed in Table 3. The *P*-values were used as a tool to check the significance of each of the coefficients, which, in turn, are necessary to understand the pattern of the mutual interactions

Table 3. **Estimated regression coefficients for the optimization of silver nanoparticles biosynthesis using central composite design**

Variables	Coefficients	Main effect	*t*-Stat	*P*-value	Confidence level (%)
Intercept	0.395	0.790	8.816	0.000	100.000
$AgNO_3$ concentration (X_1)	-0.028	-0.056	-1.259	0.227	77.279
Incubation period (X_2)	0.247	0.494	11.024	0.000	100.000
Initial pH level (X_3)	0.330	0.660	14.729	0.000	100.000
Inoculum size (X_4)	-0.053	-0.106	-2.357	0.032	96.754
X_1X_2	-0.095	-0.190	-3.469	0.003	99.657
X_1X_3	-0.013	-0.025	-0.458	0.654	34.639
X_1X_4	0.091	0.182	3.323	0.005	99.537
X_2X_3	-0.024	-0.047	-0.859	0.404	59.602
X_2X_4	-0.026	-0.053	-0.959	0.353	64.724
X_3X_4	-0.054	-0.108	-1.966	0.068	93.189
X_1X_1	0.011	0.022	0.524	0.608	39.235
X_2X_2	0.095	0.190	4.533	0.000	99.960
X_3X_3	0.119	0.238	5.684	0.000	99.996
X_4X_4	0.000	0.000	0.000	1.000	0.039

t-student's test; *P*, corresponding level of significance

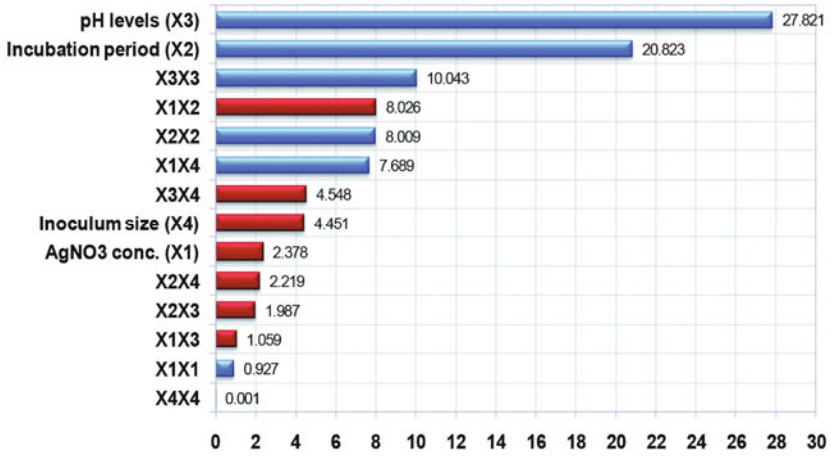

Fig. 3. **Pareto chart illustrates the order of significance of the variables affecting the silver nanoparticles biosynthesis by *S. viridochromogenes* [the blue colour represent positive effects and the red colour represent negative effects; Ranks (%) values ranging from 0.001 to 27.821].**

between the test variables. Interpretation of the data was based on the signs (positive or negative effect on the response) and statistical significance of coefficients ($P<0.05$). Interactions between two factors could appear as an antagonistic effect (negative coefficient) or as a synergistic effect (positive coefficient). It can be seen from the degree of significance that the linear effects of X_2 (incubation period), X_3 (initial pH), and X_4 (inoculum size) and quadratic effects of X_2 (incubation period) and X_3 (initial pH) are significant, meaning that they can act as limiting factors, and little variation in their value will alter the production rate. Furthermore, the probability values of the coefficient suggest that among the four variables studied, X_1 ($AgNO_3$ concentration) and X_2 (incubation period) show maximum interaction between the two variables (0.003), indicating that 99.657% of the model is affected by these variables; followed by interaction between X_1 ($AgNO_3$ concentration) and X_4 (inoculum size) (0.005), and then by the interaction between X_3 and X_4. On the other hand, among the different interactions, interactions between X_1 ($AgNO_3$ concentration), X_3 (initial pH), interaction between X_2 (incubation period) and X_3 (initial pH), interaction between X_2 (incubation period) and X_4 (inoculum size), as well as linear and quadratic effects of X_1 and quadratic effects of X_4 did not show significant effects on silver nanoparticles biosynthesis.

In order to evaluate the relationship between dependent and independent variables, and to determine the maximum silver nanoparticles biosynthesis corresponding to the optimum levels of $AgNO_3$ concentration (X_1), incubation period (X_2), initial pH (X_3), and inoculum size (X_4), a second-order polynomial model (Equation3) was proposed to calculate the optimum levels of these variables. By applying multiple regression analysis to experimental data, the second-order polynomial equation that defines the predicted response (Y) in terms of the independent variables (X_1, X_2, X_3, and X_4) was obtained:

$$Y_{(\text{Silver nanoparticles biosynthesis})} = 0.395 - 0.028X_1 + 0.247X_2 + 0.330X_3 - 0.053X_4 - 0.095X_1X_2 - 0.013X_1X_3 + 0.091X_1X_4 - 0.024X_2X_3 - 0.026X_2X_4 - 0.054X_3X_4 + 0.011X_1^2 + 0.095X_2^2 + 0.119X_3^2 + 0.000X_4^2 \quad \text{Equation (3)}$$

Where Y is the predicted response, X_1 is the coded value of $AgNO_3$ concentration, X_2 is the coded value of incubation period, X_3 is the coded value of initial pH and X_4 is the coded value of inoculum size.

The Pareto chart (Fig. 3) illustrates the order of significance of the variables affecting silver nanoparticles biosynthesis in central composite design. Among the 4 variables, the linear effects of initial pH showed the highest positive significance by 27.821%. Next to linear effect of initial pH, linear effect of incubation period and quadratic effect of initial pH showed positive effects of 20.823% and 10.026%, respectively. Interaction between $AgNO_3$ concentration and initial pH showed the higher negative effect by 1.059%.

Usually, it is necessary to check the fitted model to ensure that it provides an adequate approximation to the real system. Unless the model shows an adequate fit, proceeding with the investigation and optimization of the fitted response surface is likely give poor or misleading results. Figure 4A shows the normal probability plot of the residuals, which is an important diagnostic tool to detect and explain the systematic departures from the assumptions. The residuals were plotted against expected normal values of the model. The normal probability plot of the residuals shows the points close to a diagonal line; therefore, the errors are normally distributed and are independent of each other, and the error variances are homogenous. This indicates that the model was well fitted with the experimental results. As the residuals from the fitted model are normally distributed, all the major assumptions of the model have been validated. Figure 4B presents a plot of predicted vs. observed values of response, showing a satisfactory correlation between the experimented values and predicted values. The points gathered around the diagonal line indicate the good fit of the model. The residual plot in Fig. 4C shows equal scatter of the residual data above and below the x-axis, indicating that the variance was independent of silver nanoparticles biosynthesis, thus, supporting the adequacy of the model fit.

The interaction effects and optimal levels of the variables were determined by plotting the response surface curves (shown in Figs. 5A–5F) when one of the variables is fixed at the optimum value and the other two are allowed to vary. Figure 5A represents the interaction between $AgNO_3$ con-

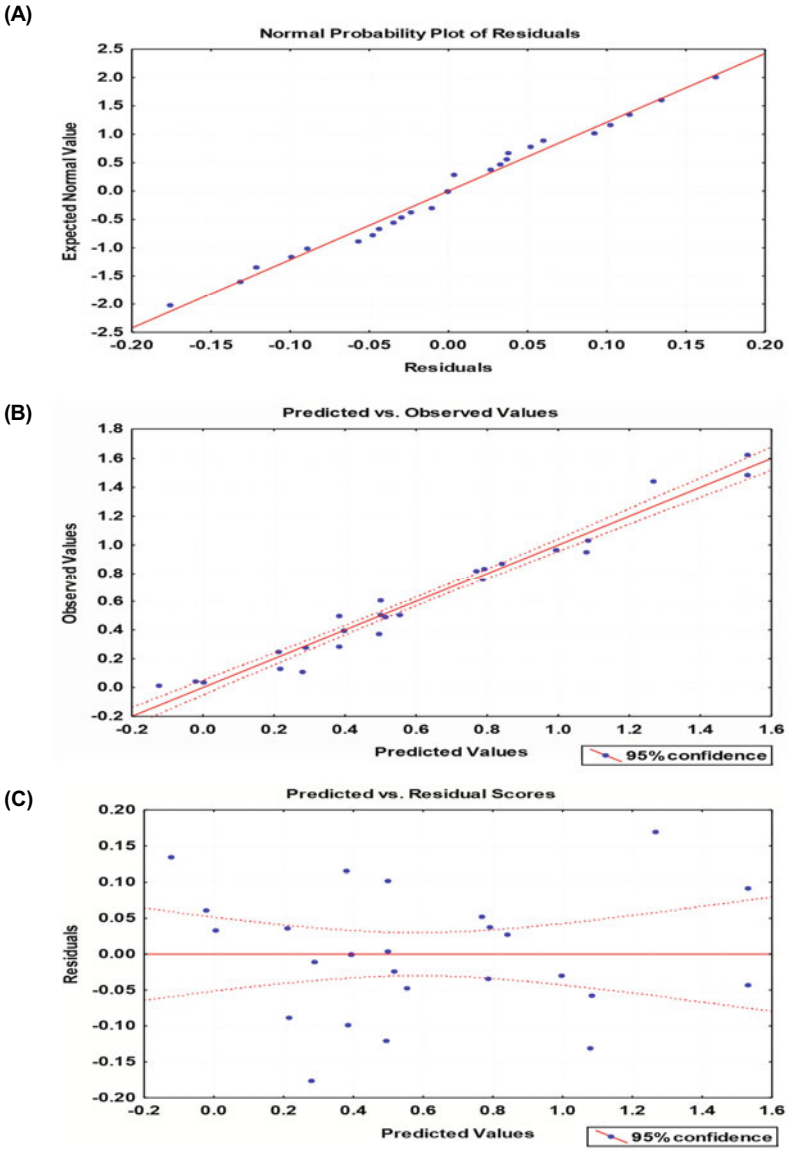

Fig. 4. (A) The normal probability plot of the residuals. (B) Correlation between the experimented and predicted values for silver nanoparticles biosynthesis of *S. viridochromogenes*, as determined by the second-order polynomial equation. (C) Plot of residuals against predicted values for silver nanoparticles biosynthesis.

centration and incubation time. It showed that the maximum silver nanoparticles yield appeared at high levels of incubation time. Lower levels of $AgNO_3$ concentration support high levels of silver nanoparticle yield, and further increase in the $AgNO_3$ concentration led to a gradual decrease in silver nanoparticles biosynthesis. Figure 5B shows that higher levels of pH support high silver nanoparticles yield. On the other hand, the maximum silver nanoparticles biosynthesis clearly situated at lower levels of $AgNO_3$ concentrations. Further increases in the concentration of $AgNO_3$ led to the gradual decrease in the production of silver nanoparticles. Figure 5C represents the interaction between $AgNO_3$ concentration and inoculum size. It showed that low level of inoculum size and $AgNO_3$ concentration supported high silver nanoparticles yield, and further increases in the inoculum size or $AgNO_3$ concentration led to a decrease in the silver nanoparticles biosynthesis. Figure 5D represents the three dimensional plot as function of pH and incubation time on silver nanoparticles biosynthesis. It was observed that there is a gradual increasing in silver nanoparticles biosynthesis through increasing both pH and incubation time. The maximum silver nanoparticles yield appeared at high levels of both pH and incubation time. Figure 5E depicts the interaction of incubation time and inoculum size. The plot reveals that the low level of inoculum size and high level of incubation time supported a high silver nanoparticles yield. Figure 5F is a three dimensional plot of the effects of pH and inoculum size on silver nanoparticles biosynthesis. According to the plot, an initial alkaline pH caused maximum silver nanoparticles biosynthesis with low level of inoculum. The biosynthesis was decreased remarkably as pH decreased. While further increases in the inoculum size resulted in a gradual decrease in silver nanoparticles yield.

Low inoculum may require longer time for microbial multiplication and substrate utilization to produce the desired product. On the other hand, high inoculum would ensure rapid proliferation of the microbial biomass. So, a balance between the proliferating biomass and substrate utilization

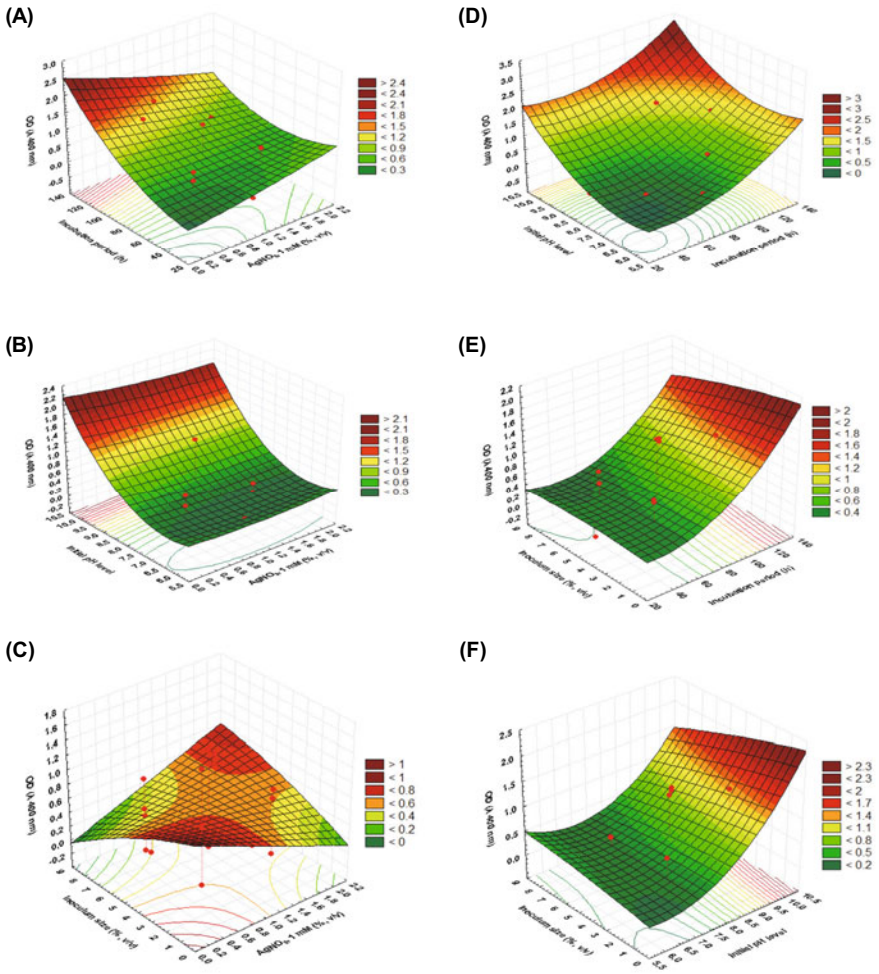

Fig. 5. Three-dimensional response surface plots (A–F) showing the interactive effects of independent variables: $AgNO_3$, 1 mM (%, v/v), incubation period (h), initial pH level, inoculum size (%, v/v) on biosynthesis of silver nanoparticles.

should yield maximum activity, as recorded by Ramachandran *et al.* (2004). As the concentration of inoculum increases, it is followed by an increase in cell mass, and after a certain period, metabolic waste interferes with the production of metabolites, which causes degradation of the product. A lower inoculum density may reduce product formation, whereas a higher inoculum may lead to poor product formation, especially due to the large accumulation of toxic substances, and the reduction of dissolved oxygen and nutrient depletion in the culture media (Rahman *et al.*, 2005). The pH of the cultivation medium is very important for the growth of microorganisms and characteristic of their metabolism, and hence, for the biosynthesis of metabolites. The hydrogen ion concentration may have a direct effect on the cell, or it may indirectly affect it by varying the dissociation degree of the medium components.

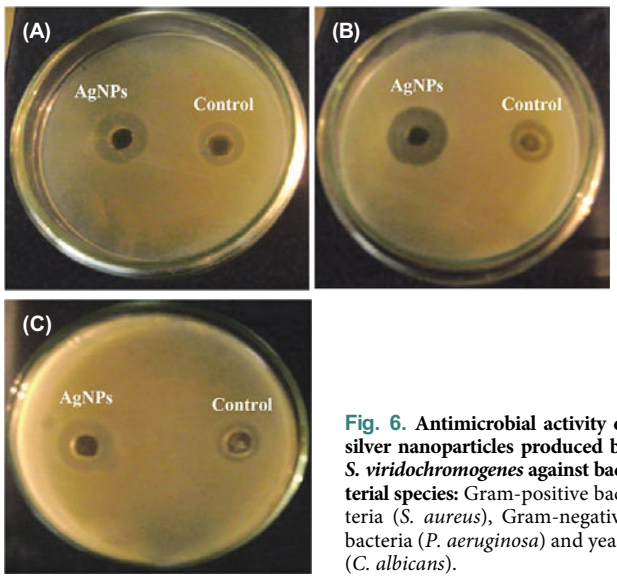

Fig. 6. Antimicrobial activity of silver nanoparticles produced by *S. viridochromogenes* against bacterial species: Gram-positive bacteria (*S. aureus*), Gram-negative bacteria (*P. aeruginosa*) and yeast (*C. albicans*).

Verification of the model

Optimal concentrations of the factors obtained from the op-

Table 4. Antimicrobial activity of silver nanoparticles produced by *S. viridochromogenes* against: Gram-positive bacteria (*S. aureus*), Gram-negative bacteria (*P. aeruginosa*) and yeast (*C. albicans*).

Microorganism	Inhibition zone diameter (mm)	
	Cell-free supernatant (before addition of $AgNO_3$)	After addition of $AgNO_3$
Staphylococcus aureus	13	20
Pseudomonas aeuroginosa	15	30
Candida albicans	15	25

timization experiment were verified experimentally and are compared with the predicted data. The measured AgNPs value was 3.5, where the predicted value from the polynomial model was 3.63. The verification revealed a high degree of accuracy of the model (more than 96.41%), indicating the model validation under the tested conditions. The optimal levels of the process variables for biosynthesis of silver nanoparticles by *S. viridochromogenes* were 0.2%, (v/v) of 1 mM $AgNO_3$, incubation period (120 h), initial pH (10) and inoculum size (1%, v/v).

Antimicrobial activity of synthesized AgNPs

In this study, the antimicrobial activity of fabricated AgNPs was evaluated against Gram-positive (*S. aureus*), Gram-negative (*P. aeruginosa*) bacterial strains and yeast (*C. albicans*) by the well diffusion method (Fig. 6). A control (cell-free fermentation broth without $AgNO_3$ addition) was also maintained in each plate. The diameter of inhibition zone around each well is presented in Table 4. The highest antimicrobial activity was observed against *Pseudomonas aeruginosa,* whereas a lower activity was found against *S. aureus*. These findings are in agreement with those of previous studies which examined the antimicrobial activity of AgNPs against *S. aureus* (Shahverdi *et al.*, 2007).

The antibacterial potency of silver is directly proportional to the concentration of silver ions in solution (Lansdown, 2006). There are different theories proposed to evaluate the mechanism of action of AgNPs. Matsumura *et al.* (2003) proposed that silver ions interact with the thiol groups of some of the major enzymes and inactivate them. Silver ions exhibit an oligodynamic effect by denaturing the cellular proteins, inhibition of DNA replication, and alteration cell membrane permeability (Feng *et al.*, 2000). Their other studies showed that there were some structural changes in the cell membrane due to silver ions, which was responsible for the antibacterial activity of the AgNPs. The antibacterial properties of AgNPs have been attributed to the ability of the AgNPs to anchor and penetrate the bacterial cell wall and to modulate cellular signaling (Braydich-Stolle *et al.*, 2005). The major mechanism through which silver nanoparticles manifested antibacterial efficacy is by anchoring to, and penetrating the bacterial cell wall, and possibly cause further

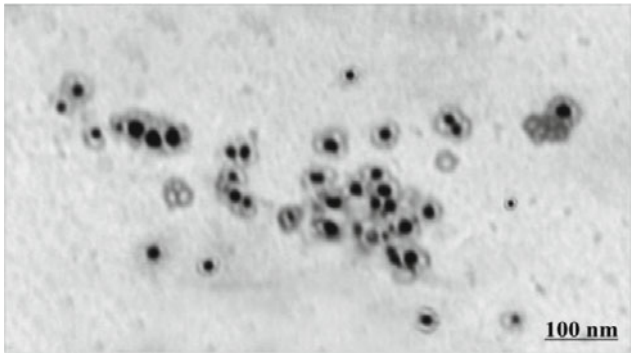

Fig. 7. Transmission electron microscopy image of produced spherical silver nanoparticles using culture supernatant of *S. viridochromogenes*. Scale bar = 100 nm.

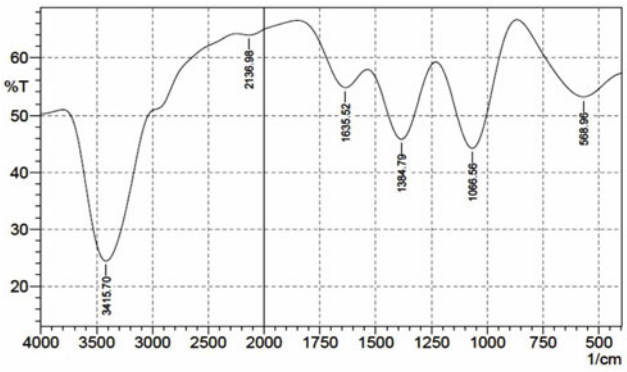

Fig. 8. FTIR spectrum recorded by making KBr disc with synthesized silver nanoparticles by *S. viridochromogenes*.

damage by interacting with sulphur and phosphorus containing compounds, including DNA (Singh *et al.*, 2008). The synthesized AgNPs with smaller size can drastically affect the cell membrane and further interact with DNA, and causes inhibition of DNA replication (Morones *et al.*, 2005), causing depletion of intracellular ATP by rupture of plasma membrane or by blocking respiration in association with oxygen and sulfhydryl (S H) groups on the cell wall, to form disulfide (R S S R) bonds, thereby leading to cell death (Kumar *et al.*, 2004).

Characterization of AgNPs by transmission electron microscopy (TEM)

Transmission electron microscopy analysis was carried out to determine the morphology and size of the AgNPs. TEM analysis showed the formation of well dispersed spherical silver nanoparticles, the size of AgNPs in the range of 2.15–7.27 nm (Fig. 7). The shape of AgNPs, predominantly spherical in shape, is common to microbial mediated synthesis (Shivaji *et al.*, 2011).

Fourier Transform Infrared (FTIR) analysis

FTIR spectroscopy was used to characterize the surface chemistry of silver nanoparticles. The FTIR measurement

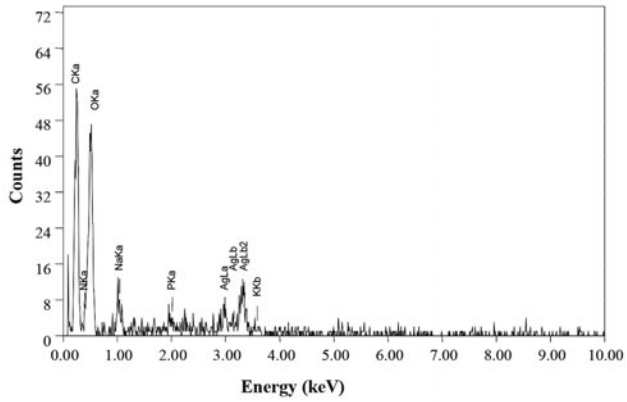

Fig. 9. EDX spectrum recorded showing peak between 3 and 4 keV, confirming the presence of silver.

can also be utilized to study the presence of protein molecules in the solution. Figure 8 shows the FTIR spectrum recorded by making KBr disc with synthesized silver nanoparticles by *S. viridochromogenes*. The spectrum shows the presence of six bands. The presence of bands at 1066.56 cm^{-1} in the FTIR spectra is attributed to C-O stretching vibration (Chao *et al.*, 2012). The FTIR band at 1384 cm^{-1} corresponded to C=C stretching of an aromatic amine group or C-N stretching vibrations of aromatic amines (Faramarzi and Forootanfar, 2011), suggested that the capping agent of biosynthesized nanoparticles possesses an aromatic amine group. In addition, the presence of bands at 1635 and 2136 Cm^{-1} in the FTIR spectra are attributed to -C=O stretching vibrations in amide linkages (amide II) of protein present in bacterial supernatant (Kovnir *et al.*, 2009; Hudlikar *et al.*, 2012). The band seen at 3415 cm^{-1} is typical of the stretching vibration mode of O–H stretching vibrations (Das *et al.*, 2006). This type of FTIR spectra supports the presence of a protein type of compound on the surface of biosynthesized nanoparticles, confirming that metabolically produced proteins acted as capping agents during production, and prevented the reduced silver particle agglomeration. In fact, the carbonyl groups from amino acid residues, as well as those from peptides of proteins, are known for their strong silver binding properties. It has been suggested that the stability of the AgNPs generated using cell-free culture supernatants could be due to the presence of a proteinaceous capping agent that prevents aggregation of the nanoparticles (Saifuddin *et al.*, 2009).

Energy-dispersive X-ray spectroscopy

Energy-dispersive X-ray spectroscopy (EDX) is an analytical technique which is used for the elemental analysis or chemical characterization of a sample. In the current study, for the confirmation of AgNPs, EDX spectroscopy analysis was performed, which confirmed the presence of elemental silver by the signals (Fig. 9). The optical absorption band peak in the range of 3 to 4 keV is typical for the absorption of metallic silver nanocrystallites (Magudapathy *et al.*, 2001). However; there were other EDX peaks for Na, P and K, suggesting that they were mixed precipitates from the centrifuged cell free supernatant.

Conclusion

In this study, we demonstrated the green extracellular synthesis of spherical shaped silver nanoparticles when the cell free culture supernatant of the *Streptomyces viridochromogenes* was treated with 1 mM silver nitrate. The silver nanoparticles thus formed were characterized by UV–Vis spectroscopy, TEM, FTIR and EDX. The synthesized AgNPs were found to be spherical in shape, and the particle sizes were in the range of 2.15–7.27 nm. UV–visible absorbance spectral analysis confirmed the single surface plasmon resonance at 400 nm of biosynthesized AgNPs. Furthermore, the biosynthesized AgNPs displayed a pronounced antimicrobial activity against different clinically important pathogenic microorganisms. The outcomes indicated an increased antimicrobial activity for the biosynthesized AgNPs compared to the cell-free filtrate alone. The FTIR study suggests that the protein might have played an important role in the stabilization of silver nanoparticles, through the coating of a protein moiety on the nanosilver particles.

References

Ahmad, N., Sharma, S., Alam, M.K., Singh, V.N., Shamsi, S.F., Mehta, B.R., and Fatma, A. 2010. Rapid synthesis of silver nanoparticles using dried medicinal plant of basil. *Colloids Surf. B Biointerfaces* **81**, 81–86.

Ahmad, A., Mukherjee, P., Senapati, S., Mandal, D., Khan, M.I., Kumar, R., and Sastry, M. 2003. Extracellular biosynthesis of silver nanoparticles using the fungus *Fusarium oxysporum*. *Colloids Surf. B.* **28**, 313–318.

Akaighe, N., MacCuspie, R.I., Navarro, D.A., Aga, D.S., Banerjee, S., Sohn, M., and Sharma, V.K. 2011. Humic acid-induced silver nanoparticle formation under environmentally relevant conditions. *Environ. Sci. Technol.* **45**, 3895–3901.

Akhnazarova, S. and Kafarov, V. 1982. Experiment optimization in chemistry and chemical engineering. Mir Publishers. Moscow.

Box, G.E.P., Hunter, W.G., and Hunter, J.S. 1978. Hunter. Statistics for experiments. pp. 291–334. John Wiley and Sons. New York, USA.

Brause, R., Moeltgen, H., and Kleinermanns, K. 2002. Characterization of laser ablated and chemically reduced silver colloids in aqueous solution by UV/Vis spectroscopy and STM/SEM microscopy. *Appl. Phys. B* **75**, 711–716.

Braydich-Stolle, L., Hussain, S., Schlager, J.J., and Hofmann M.C. 2005. *In vitro* cytotoxicity of nanoparticles in mammalian germline stem cells. *Toxicol Sci.* **88**, 412–419.

Chao, T.C., Song, G.X., Hansmeier, N., Westerhoff, P., Herckes, P., and Halden, R.U. 2012. Characterization and LC-MS/MS based quantification of hydroxylated fullerenes. *Anal. Chem.* **83**, 1777–1783.

Chen, X.C., Bai, J.X., Cao, J.M., Li, Z.J., Xiong, J., Zhang, L., Hong, Y., and Ying, H.J. 2009. Medium optimization for the production of cyclic adenosine 3′, 5′-monophosphate by *Microbacterium* sp. no. 205 using response surface methodology. *Bioresour. Technol.* **100**, 919–924.

Das, S., Kar, S., and Chaudhuri, S. 2006. Optical properties of SnO_2 nanoparticles and nanorods synthesized by solvothermal process. *J. Appl. Phys*. **99**, 114303(1-7).

Djekrif-Dakhmouche, S., Gheribi-Aoulmi, Z., Meraihi, Z., and Bennamoun, L. 2006. Application of a statistical design to the optimization of culture medium for a-amylase production by *Aspergillus niger* ATCC 16404 grown on orange waste powder. *J. Food Eng.* **73**, 190–197.

Elibol, M. 2004. Optimization of medium composition for actinorhodin production by *Streptomyces coelicolor* A3 (2) with response surface methodology. *Process Biochem.* **39**, 1057–1062.

El-Naggar, N.E., Sherief, A.A., and Hamza, S.S. 2011. Bioconversion process of rice straw by thermotolerant cellulolytic *Streptomyces viridiochromogenes* under solid-state fermentation conditions for bioethanol production. *Afr. J. Biotechnol.* **10**, 11998–12011.

Faramarzi, M.A. and Forootanfar, H. 2011. Biosynthesis and characterization of gold nanoparticles produced by laccase from *Paraconiothyrium variabile*. *Colloids Surf. B Biointerfaces* **87**, 23–27.

Feng, Q.L., Wu, J., Chen, G.Q., Cui, F.Z., Kim, T.N., and Kim, J.O. 2000. A mechanistic study of the antibacterial effect of silver ions on *Escherichia coli* and *Staphylococcus aureus*. *J. Biomed. Mater. Res.* **52**, 662–668.

Ganesh Babu, M.M. and Gunasekaran, P. 2009. Production and

structural characterization of crystalline silver nanoparticles from *Bacillus cereus* isolate. *Colloids Surf. B Biointerfaces* **74**, 191–195.

Hemanth Naveen, K., Gaurav Kumar, S., Karthik, L., and Bhaskara Rao, K.V. 2010. Extracellular biosynthesis of silver nanoparticles using the filamentous fungus *Penicillium* sp. *Arch. Appl. Sci. Res.* **2**, 161–167.

Hudlikar, M., Joglekar, S., Dhaygude, M., and Kodam, K. 2012. Latex-mediated synthesis of ZnS nanoparticles: green synthesis approach. *J. Nano. Res.* **14**, 1–6.

Kalimuthu, K., Suresh Babu, R., Venkataraman, D., Bilal, M., and Gurunathan, S. 2008. Biosynthesis of silver nanocrystals by *Bacillus licheniformis*. *Colloids Surf. B*. **65**, 150–153.

Kalishwaralal, K., Banumathi, E., Pandian, S.B.R.K., Deepak, V., Muniyandi, J., and Eom, S.H. 2009. Silver nanoparticles inhibit VEGF induced cell proliferation and mgration in bovine retinal endothelial cells. *Colloids Surf. B.* **73**, 51–57.

Kalishwaralal, K., Deepak, V., Pandian, S.R.K., Kottaisamy, M., Manikanth, S.B., Karthikeyan, B., and Gurunathan, S. 2010. Biosynthesis of silver and gold nanoparticles using *Brevibacterium casei*. *Colloids Surf. B. Biointerfaces* **77**, 257–262.

Kaushik, R., Saran, S., Isar, J., and Saxena, R.K. 2006. Statistical optimization of medium components and growth conditions by response surface methodology to enhance lipase production by *Aspergillus carneus*. *J. Mol. Catal B-Enzyme* **40**, 121–126.

Kovnir, K., Armbrüster, M., Teschner, D., Venkov, T.V., Szentmiklósi, L., Jentoft, F.C., Grin, Y., and Schlogl, R. 2009. *In situ* surface characterization of the intermetallic compound PdGa. A highly selective hydrogenation catalyst. *Surf. Sci.* **603**, 1784–1792.

Krishnaraj, C., Jagan, E.G., Rajasekar, S., Selvakumar, P., Kalaichelvan, P.T., and Mohan, N. 2010. Synthesis of silver nanoparticles using *Acalypha indica* leaf extracts and its antibacterial activity against water borne pathogens. *Colloids Surf. B Biointerfaces* **76**, 50–56.

Kumar, V.S., Nagaraja, B.M., Shashikala, V., Padmasri, A.H., Madhavendra, S.S., and Raju, B.D. 2004. Highly efficient Ag/C catalyst prepared by electro-chemical deposition method in controlling microorganisms in water. *J. Mol. Catal. A.* **223**, 313–319.

Lansdown, A.B. 2006. Silver in health care: antimicrobial effects and safety in use. *Curr. Probl. Dermatol.* **33**, 17–34.

Magudapathy, P., Gangopadhyay, P., Panigrahi, B.K., Nair, K.G.M., and Dhara, S. 2001. Electrical transport studies of Ag nanocrystallites embedded in glass matrix. *Physics B.* **299**, 142–146.

Matsumura, Y., Yoshikata, K., Kunisaki, S., and Tsuchido, T. 2003. Mode of bactericidal action of silver zeolite and its comparison with that of silver nitrate. *Appl. Envir. Microbiol.* **69**, 4278–4281.

Mie, G. 1908. Beiträge zur Optik trüber Medien, speziell kolloidaler Metallösungen. *Ann. Phys.* **25**, 377–445.

Minaeian, S., Shahverdi, A.R., Nohi, A.S., and Shahverdi, H.R. 2008. Extracellular biosynthesis of silver nanoparticles by some bacteria. *J. Sci. I.A.U.* **17**, 1–4.

Mohanpuria, P., Rana, K.N., and SYadav, K. 2008. Biosynthesis of nanoparticles: technological concepts and future applications. *J. Nanopart. Res.* **10**, 507–517.

Montgomery, D.C. 1991. Design and analysis of experiments. Wiley, New York, USA.

Morones, J.R., Elechiguerra, J.L., Camacho, A., Holt, K., Kouri, J.B., Ramirez, J.T., and Yacaman, M.J. 2005. The bactericidal effect of silver nanoparticles. *Nanotech.* **16**, 2346–2353.

Natarajan, K., Subbalaxmi, S., and Ramachandra Murthy, V. 2010. Microbial production of silver nanoparticles. *Digest. J. Nanomater. Biostruc.* **5**, 135–140.

Panwal, J.H., Viruthagiri, T., and Baskar, G. 2011. Statistical modeling and optimization of enzymatic milk fat splitting by soybean lecithin using response surface methodology. *Inter. J. Nutri. Metabol.* **3**, 50–57.

Rahman, R.N.Z.A., Lee, P.G., Basri, M., and Salleh, A.B. 2005. Physical factors affecting the production of organic solvent-tolerant protease by *Pseudomonas aeruginosa* strain K. *Bioresour. Technol.* **96**, 429–436.

Rai, M., Yadav, A., and Gade, A. 2009. Silver nanoparticles as a new generation of antimicrobials. *Biotechnol. Adv.* **27**, 76–83.

Ramachandran, S., Patel, A.K., Nampoothiri, K.M., Francis, F., Nagy, V., Szakacs, G., and Pandey, A. 2004. Coconut oil cake: A potential raw material for the production of α-amylase. *Bioresour. Technol.* **93**, 169–174.

Saifuddin, N., Wong, C.W., and Nur Yasumira, A.A. 2009. Rapid biosynthesis of silver nanoparticles using culture supernatant of bacteria with microwave irradiation. *J. Chem*. **6**, 61–70.

Sanghi, R. and Verma, P. 2009. Biomimetic synthesis and characterisation of protein capped silver nanoparticles. *Biores. Technol.* **100**, 501–504.

Senapati, S., Ahmad, A., Khan, M.I., Sastry, M., and Kumar, R. 2005. Extracellular biosynthesis of bimetallic Au-Ag alloy nanoparticles. *Small.* **1**, 517–520.

Shahverdi, R.A., Fakhimi, A., Shahverdi, H.R., and Minaian, S. 2007. Synthesis and effect of silver nanoparticles on the antibacterial activity of different antibiotics against *Staphyloccocus aureus* and *Escherichia coli*. *Nanomedicine* **2**, 168-171

Shivaji, S., Madhu, S., and Singh, S. 2011. Extracellular synthesis of antibacterial silver nanoparticles using psychrophilic bacteria. *Process Biochem.* **46**, 1800–1807.

Singh, M., Singh, S., Prasad, S., and Gambhir, I.S. 2008. Nanotechnology in medicine and antibacterial effect of silver nanoparticles. *Dig. J. Nanomater. Biostruct.* **3**, 115–122.

Sosa, I.O., Noguez, C., and Barrera, R.G. 2003. Optical properties of metal nanoparticles with arbitrary shapes. *J. Phys. Chem.* **107**, 6269–6275.

Souza, G.I.H., Marcato, P.D., Durán, N., and Esposito, E. 2004. Utilization of *Fusarium oxysporum* in the biosynthesis of silver nanoparticles and its antibacterial activities. *In* IX National Meeting of Environmental Microbiology. Curtiba, Brazil.

Tang, Y.X., Subramaniam, V.P., Lau, T.H., Lai, Y.K., Gong, D.G., Kanhere, P.D., Cheng, Y.H., Chen, Z., and Dong, Z.L. 2011. *In situ* formation of large-scale Ag/AgCl nanoparticles on layered titanate honeycomb by gas phase reaction for visible light degradation of phenol solution. *Appl. Catal. B: Environmental*. **106**, 577–585.

Vaidyanathan, R., Gopalram, S., Kalishwaralal, K., Deepak, V., Pandian, S.R.K., and Gurunathan, S. 2010. Enhanced silver nanoparticle synthesis by optimization of nitrate reductase activity. *Colloid. Surf. B.* **75**, 335–341.

Valodkar, M., Bhadorai, A., Pohnerkar, J., Mohan, M., and Thakore, S. 2010. Morphology and antibacterial activity of carbohydrate stabilized silver nanoparticles. *Carbohydr. Res.* **345**, 1767–1773.

Verma, V.C., Kharwar, R.N., and Gange, A.C. 2009. Biosynthesis of noble metal nanoparticles and their application. CAB Review: perspectives in agriculture, Vatenary science. *Nutr. Nat. Resour.* **4**, 1–17.

Vigneshwaran, N., Arati Kathe, N., Varadarajan, P.V., Rajan Nachane, P., and Balasubramanya, R.H. 2006. Biomimetics of silver nanoparticles by white rot fungus, *Phaenerochaete chrysosporium*. *Colloids Surf. B. Interfaces* **53**, 55–59.

Waksman, S.A. 1959. Strain specificity and production of antibiotic substance. X. Characterization and classification of species within the *Streptomyces griseus* group. *Proc. Natl. Acad. Sci. USA* **45**, 1043–1047.

Wenster-Botz, D. 2000. Experimental design for fermentation media development: Statistical design or global random search? *J. Biosci. Bioeng.* **90**, 473–483.